Defence Science Journal, Vol. 69, No. 5, September 2019, pp. 489-494, DOI : 10.14429/dsj.69.13338

Failure Behaviours of Steel Projectiles with Localised Melting Against Armour Plates

Zhengxiang Shen[#,*], Hu Chen[#], Du Wang[#], Shuqiang Yuan[@], Dingyue Chen[#], and Guorong Zhu[#]

[#]*Port-Neighboring Equipment Safety Assessment Center, Ningbo Special Equipment Inspection & Research Institute, Ningbo - 315 048, PR China*

[@]*NingBo Institute,China North Material Science and Engineering Technology Group, Ningbo - 315 103, PR China*

[*]*E-mail: shenzx0403@126.com*

ABSTRACT

The surface remelting technology of high energy beam can locally weaken the case for controlled fragmentation, which may affect the survivability of the impacting projectiles. Failure behaviours of steel projectiles with melted layers grid normally perforating armour plates was investigated. The results reveal that shear fracture mainly occurs in the nose region of projectiles due to high loading, and the melting zone of projectiles can keep integrity with no damage, which means the survivability of projectile can be assured. Furthermore, an analytical model was proposed to the structural analysis of projectile, which is in accordance with the test results.

Keywords: Projectile; Localised melting; Failure; Mass loss; Magnetic particle inspection

1. INTRODUCTION

The impact and protection engineering has become one of the key issues in the design of weapons. Nevertheless, most researchers pay more attention to the performance of targets under impact loading, the deformation and fracture of projectiles under extreme conditions need to be studied deeper. In the previous studies, considering the complexity of impacting, the rigid target hypothesis was often used. The classical Taylor bar impact test is a typical representative of this aspect. Backman & Goldsmith[1], Woodward[2], *et al*. and Rakvåg[3], *et al*. have revealed various typical failure modes of projectile bodies. In some special cases, the hydrostatic tension can also cause many detects and serious destruction to the projectile body.

A systematic research on the steel projectile impacting harder target was performed by Chen[4], *et al*., which is different from the standard test of Taylor bar to some degree. For example, the deformation zone of projectile head comprises: an inside circle and an outside ring, the tensile cracking in the outside ring never passes through the interface of these two portions. Ren[5], *et al*. studied the fracture surface of recovered projectile by scanning electron microscope in which the spiral shear crack was symmetrically self-organised. Xiao[6], *et al*. performed impacting experiments with two kinds of projectiles, the soft projectile were fractured in the petal type, while the hard were fragmented. Besides, the loop patterns also appeared at the nose of projectile. Despite all this, the researches on the failure behaviours of impacting projectile are still insufficient.

With regard to the structural optimisation of penetrating projectiles, the damage ability of warhead perforated target is of special interest. There is a recognised need for controlled fragmentation methods for warheads of projectiles against hard targets. The local melting on the case by high energy beam is one of the innovative technologies of fragmentation[7]. However, since the melted layers grid formed into the outer surface of the case, may act as a stress-raiser during impacting process, there is a concern that the presence of such a grid might affect the structural integrity of the case and the survivability of the projectile.

This study is to investigate the failure behaviours of steel localised melting projectiles perforated armour steel plates, and the possible effect of melted layers grid on the survivability of the steel projectiles was also examined. Firstly, experiments of small-scale, hollow steel projectiles of local melting normally impacting armour steel plates were conducted, and metallographic examinations were made to reveal the deformation and fracture mode of selected residual projectiles. Secondly, the magnetic particle inspection is selected to examine the main structure of projectiles. At last, an analytical model is introduced and discussed.

2. EXPERIMENTAL PROCEDURES

2.1 System of Experiment

The simulated projectiles were shot at the target plates by 37 mm smooth bore gun at the range of 380~500 m/s. To minimise the speed error as possible, the mass of internal charge was accurately evaluated. Some aluminum foils and a multi-channel time-measuring system HG 202C were put up to provide signals for the time recorder at the trajectory of projectile. Furthermore, a high speed camera Photron SA5

Received : 17 July 2018, Revised : 01 May 2019
Accepted : 30 May 2019, Online published : 17 September 2019

was set to capture the flight attitude and impacting process of projectile. Some wood blocks placed behind the target plate were employed to recover projectile for eliminating the secondary damage effect. The main experimental devices and principle are shown in Fig. 1. The magnetic particle inspection was carried on by CEW-4000 AC/DC dual-purpose magnetic particle testing machine, and the oil-based magnetic suspension was applied to the recovered projectiles by pouring or impregnation, to ensure that the surface of the shell is completely covered.

2.2 Projectile and Target Plate

The material of projectile was 30CrMnSiNi2A steel, and the main compositions were seen in Table 1. The projectiles were machined with an oval shape (CRH=3.0), and the overall length is 102 mm. To meet the requirement of speed, a hollow structure is adopted to reduce the launching weight, as shown in Fig. 2. All projectiles are pre-heat treated to make Rockwell hardness up to 40. The main parameters of heat treatment were described in Table 2. The dynamic mechanical properties of 30CrMnSiNi2A steel with Split-Hopkinson pressure bar and static material test system within five strain rates were shown in Fig. 3, it is seen that the yield stress is about 1580 MPa at the strain rate of 10^{-4} s^{-1}, while that increases to 1682 MPa at 500 s^{-1} strain rate. During the increase of strain rate from 500 s^{-1} to 5000 s^{-1}, the yield stress of the material increases gradually(1682~1920 MPa), but the variation is slight. It is notable that 30CrMnSiNi2A steel is less sensitive to the strain rate.

Table 1. Nominal chemical composition of 30CrMnSiNi2A steel (wt%)

C	Si	Mn	S	P	Ni	Cr	Mo	V
0.332	1.06	1.19	0.011	0.018	1.02	1.75	<0.15	<0.05

Table 2. Heat treatment process of 30CrMnSiNi2A steel

Normalising	Cooling	Tempering	Cooling
1.5h at 900 ℃ in furnace	Oil at 900 ℃ + air	2×1.5h at 250 ℃	Air

For producing fragments of a desired size and shape, a local melted and re-solidified layers grid system was formed on the exterior surface by high energy beam. The interaction between the case and high energy beam aims to create a grid

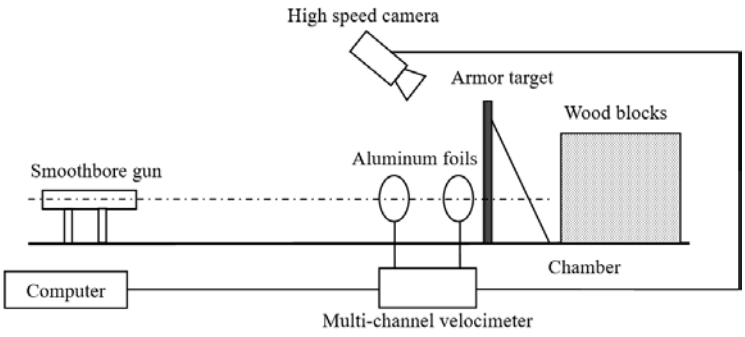

Figure 1. General view of experimental system.

(a)

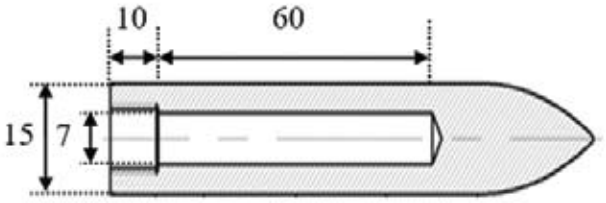

(b)

Figure 2. (a) The projectile used in the experiment (b) The geometry and dimensions in mm.

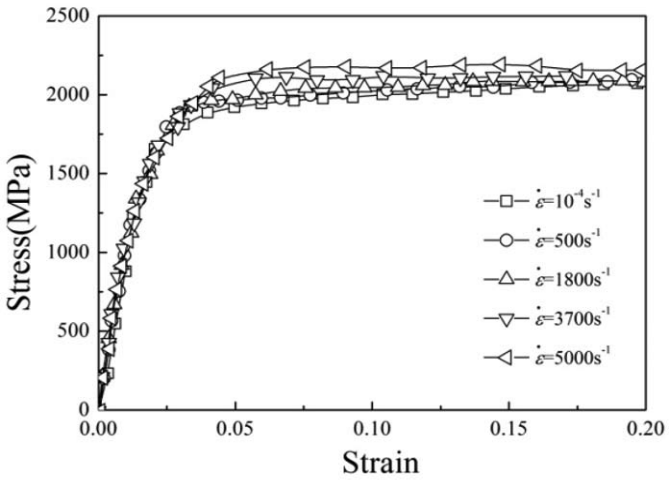

Figure 3. Compressive stress-strain curve of 30CrMnSiNi2A steel at different strain rates.

of local melted layers on the surface, as the case passes under high energy beam. Because of the self-quenching effect of the cold interior of the sample, the melted layer has usually a finer and homogeneous structure than its original bulk material. Shear fractures initiate and propagate along the melted trajectories during the expansion process of case. Thus, the fragmentation behaviour of metal is enhanced along these definite and pre-determined paths[8]. Figure 4 displays the geometry and microstructure of melted zone, at which there are two different parts. The melted layer was composed of martensite, discrete cementite particles and retained austensite. As the carbides started dissolving during the rapid heating process, austensite with high carbon content were formed. Finally, the rapid cooling of surrounding material results in the formation of martensite, carbide and

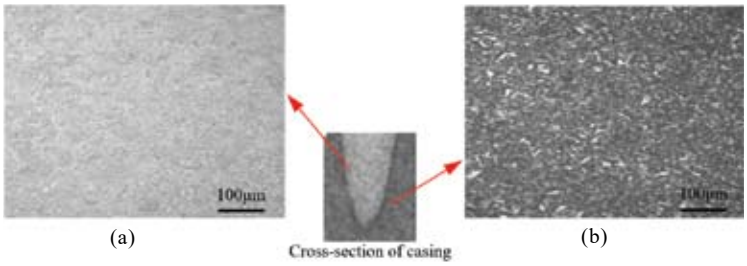

Figure 4. Microstructure of (a) Melting layer and (b) Bulk material.

retained austenite. In comparison with the bulk material, the grain has been refined remarkably. According to the results of measurement, the average value of surface hardness of the melted layer is about HRC 52.

The target plates in the experiments were manufactured from armour steel with the thicknesses of 4.0 mm and 6.0 mm, which were fixed by heavy blocks of iron. These target plates were heat-treated with the quenching and tempering processing to have a static tensile strength of 1500 MPa. In this paper, the critical processing parameter is low temperature tempering at 250 °C for 2 hours and air-cooled to the room temperature, avoiding unnecessary brittleness at the same time.

3. ANALYSIS AND DISCUSSION OF RESULTS

3.1 Summary of Results

A total of seven tests were completed and all the projectiles perforated the targets. The main conditions and results of tests are as listed in Table 3. To examine the characteristics of damage, the residual projectiles were recovered for further analysis. The failure of projectiles was described by mass loss, deformed length and diameter. Due to the plastic strain of the material in the contact zone of the projectile and target, the damage develops rapidly. All tests have been conducted under the normal penetration conditions.

3.2 Fracture Mode and Mass Loss of Projectile

During perforation of armour steel, projectiles experience high loads of short duration, which may be the primary factor for failure. The results of macroscopic inspection in Fig. 5 indicated that the integrated projectiles still maintained, instead of damage largely confining to the projectile nose.

Compared with the original, the mass loss of the residual projectile is larger and the nose cracks. Notable is the relative small amount of fracture in the nose region, which can be described in terms of velocity discontinuities identified by regions of maximum strain rate. The projectiles have only partly been destroyed, no cavities or cracks can be recognised at the unbroken part either by passage of stress relief waves or by intense friction. A typical fracture surface from the front of the projectile in perforation of targets is shown in Fig. 6. It is apparent that the dominating failure of projectile nose is shear fracture with a distinct glassy surface. For the strain rate sensitivity and tempering brittleness of 30CrMnSiNi2A steel used in this study, the nose of projectile was shear fractured with the angle of 45° by the dynamical compression load at high strain rates. Some melts are discovered at the shear plane, which can be explicated by the high temperature effect of local shear action.

The greater the impact speed, the more serious the damage, the greater the mass loss of the projectile. The maximum loss of the nose to the total mass is up to 6 per cent. Blue brittleness is also observed in the nose of some projectile, which is brought about by the spilling of secondary particles at a temperature of approximately 300 °C[9]. Generally, blue brittleness seems to coincide with the appearance of cracking[3]. It is reasonable considered that high pressure and heat generated by the transient effect between projectile and target are the main cause of shear fracture. The failure mode of target is affected by the impact velocity, strength, dimensions of nose, thickness, etc. The target plate is thinner than the projectile diameter, so the plates failed by the typical petal-like mode, under the local strong loads. It is generally believed that high radial and circumferential tensile stresses lead to this deformation[10].

In case of 6 mm thickness armour steel plate, the nose of projectile was seriously destroyed and shorter. From the SEM image of fracture surface given in Fig. 7, a flat fracture surface appears with cleavage-like patterns. This is a clear evidence of shear fracture as the dominating fracture mode. Moreover, the mass loss increases to about 8.7~8.8 % of the total mass, and the plate fails due to plugging, with the action of stretch stress. The plugs seem to be both smooth and cylindrical, which is significantly different from the failure mode of 4 mm target plate.

During impact, the plastic deformation of target plate will absorb energy. Therefore, the material flow resistance directly affects the protective performance of the plate. With the thickness increasing from 4 mm to 6 mm, the target absorbs more energy, results in the penetration resistance of projectile increasing. The difference is determined by the bending stiffness between the two plates. The bend stiffness is as[11]:

Table 3. Results of tests

Serial number	Initial velocity (m/s)	Thickness of target (mm)	Initial mass (g)	Residual mass (g)	Deformation on length (mm)	Deformation on diameter (mm)	Mass loss (per cent)
1-1	407	4	107.2	104.9	11	0.02	2.14
1-2	417	4	107.5	104.3	11.3	0.04	2.97
1-3	441	4	107.1	103.7	11.8	0.04	3.17
1-4	484	4	107.5	103.6	12	0.02	3.62
1-5	494	4	107	100.3	18	0.02	6.2
2-1	387	6	107.3	96.2	21	0.02	8.72
2-2	420	6	107.3	98	22	0.04	8.8

Figure 5. The photographs of the projectiles recovered with target of (a) 4 mm thickness and (b) 6 mm thickness.

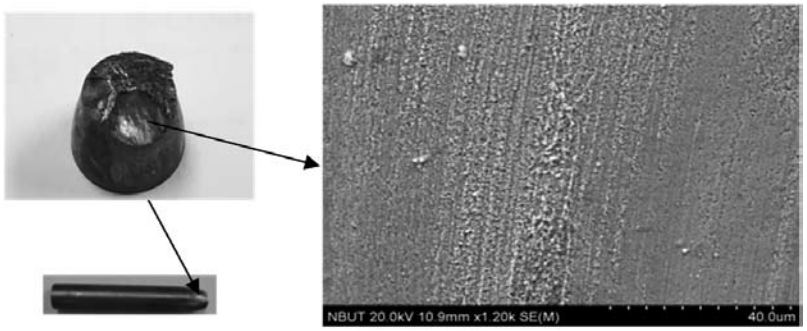

Figure 6. Microscopic image of the nose of projectile after impact (v_i = 441 m/s) on a 4 mm thick target plate.

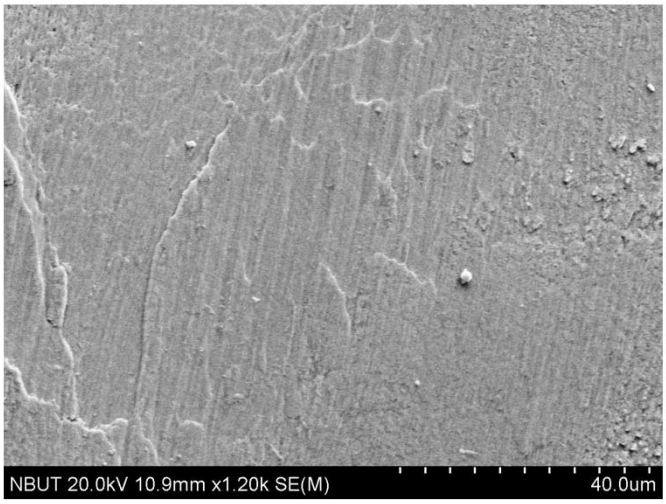

Figure 7. Surface morphology of fracture impacted at 387 m/s.

$$K = \frac{ET^3}{12\left(1-\upsilon^2\right)} \tag{1}$$

where T is the thickness of plate, E is the elastic modulus of material and υ denotes Poisson's ratio. Because the bending stiffness increases to cubic with the thickness of the plate, the ballistic resistance of 6 mm thickness plate is significantly larger than that of 4 mm thickness plate, and the damage of projectiles penetrating thin plates are smaller than that penetrating thick plates. For two types of target plates, the damage of projectile head becomes more serious with the impact velocity increasing, but no visible damage or bulge occurring at the melting location of projectiles. The nondestructive examination of the melting zone will be discussed in next.

3.3 Nondestructive Inspection

The nondestructive inspection used in this paper is to detect surface and near-surface discontinuities/cracks by magnetic flux leakage and magnetic powders. Under the effect of magnetic flux leakage, the magnetic particles assemble at discontinuity and form magnetic traces, which show the position, shape and size of discontinuity. This nondestructive method can be used to examine defects or micro-cracks in the melted zone of residual projectiles. To make these indications easy to recognise, the melting zones of projectiles are uniformly coated with small white magnetic particles (see Fig. 8). The results of inspection are analysed and processed

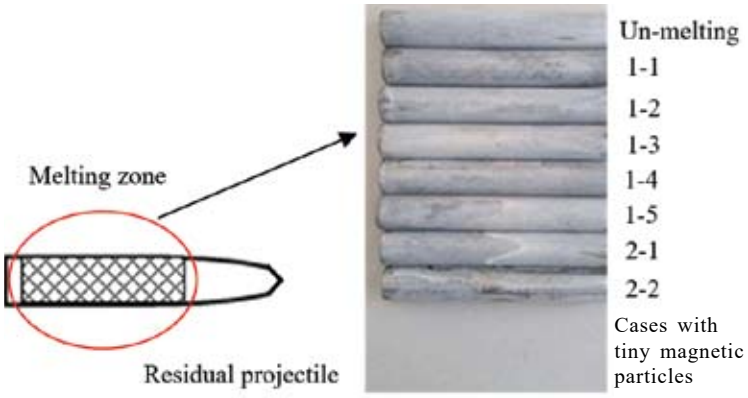

Figure 8. The projectiles structure with white magnetic particles.

as shown in Table 4, which indicate there is no damage at the melting location during impacting. It implies that the presence of melted layers grid has little effect on the structural integrity or the survivability of the projectile.

Table 4. The results of magnetic particle inspection

Specimen ID	Distortion in the magnetic flux
1-1	No
1-2	No
1-3	No
1-4	No
1-5	No
2-1	No
2-2	No

3.4 Discussion

In the process of penetrating target, the movement and damage of projectile are related to resistance[12]. When the projectile penetrates into the target at high speed, an axial compressive stress will be produced in the body. Thus, it is necessary to estimate the stress distribution of the projectile structure.

Suppose a projectile of total mass m impacts a target plate, and the resistance of projectile body is sketched in Fig. 9. The external radius is expressed by R, the internal radius is expressed by r. Regardless of the projectile nose, the length of main structure is L, and the area of cross-section at the axial x is $A(x)$. With the formation of craters, the impact resistance of projectile increases rapidly[13], so the maximum resistance is obtained by

$$F = ma \tag{2}$$

where a is the deceleration. The compressive stress of projectile body at the axial x is

$$\sigma_x = \frac{F}{A(x)} = \frac{\int_0^x \Delta m a}{A(x)} \tag{3}$$

$$A(x) = \pi(R^2 - r^2) \tag{4}$$

$$\Delta m = \rho \Delta V = \rho A(x) dx \tag{5}$$

It can be reasonably assumed that the compressive stress at the tail is $\sigma_{x=0}$, thus by Eqn (3) the compressive stress in the axial direction is

$$\sigma_x = \sigma_{x=0} + \frac{\rho a \int_0^x A(x) dx}{A(x)} = \sigma_{x=0} + \rho a \frac{R^2 x - r^2 x}{R^2 - r^2} = \sigma_{x=0} + \rho a x \tag{6}$$

where x is measured from the projectile tail to the cross-section position.

The variation of the compressive stress in projectile wall with the distance from projectile tail is shown in Fig. 10. It is shown that the compressive stress σ_x increases with the distance x increasing, and the nose of projectile must resist the maximum compressive stress. When the maximum value of σ_x equals the failure stress of the projectile material σ_{cr}, the head of the projectile will be damaged[12]. On the other hand, the integrity of local melting zone at the main structure is stable, this conclusion is in line with the results of experimental observation.

4. CONCLUSIONS

This research is carried out to investigate the failure mode of localised melting on outer case of projectiles after impacting armour steel plates, and examine the possibly lethal effect of melted layers grid on the survivability of projectiles. Due to the great resistant force by the target medium, the

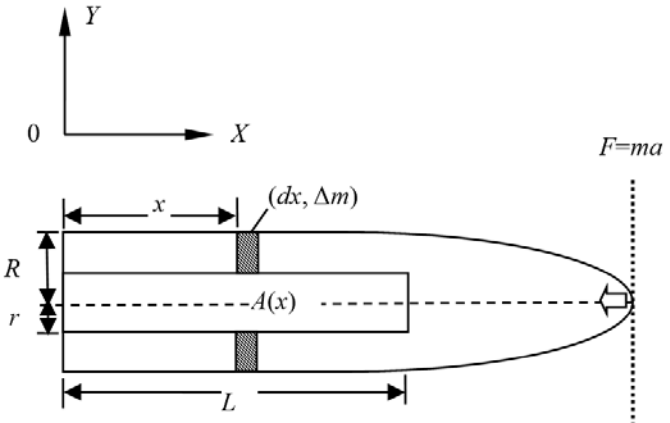

Figure 9. Schematic of projectile.

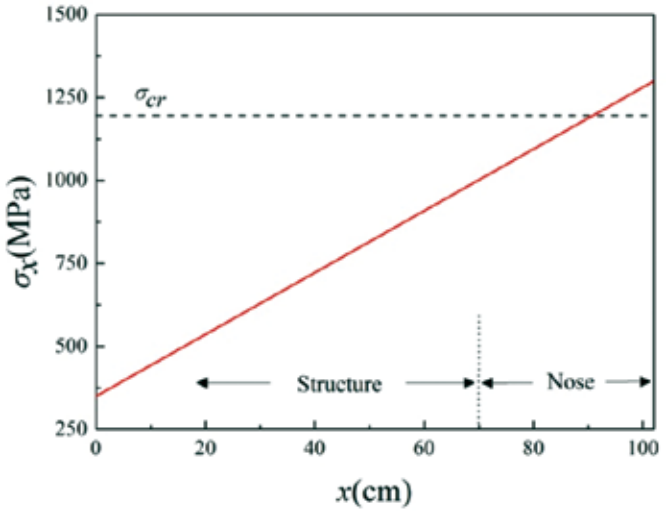

Figure 10. The variation of σ_x with x for projectile striking target plate at 407 m/s.

dominant failure mode is shear fracture acting on the nose of projectile. The examination on the residual projectiles by magnetic particle inspection indicates that there is no damage at the local melting locations, which means that the main structure of projectiles can keep integrity during impacting. An analytical model for the strength analysis of projectile structure was proposed, and the weakest location is predicted to be the nose, which meets the results of tests. From the current results, the localised melting layers has little effect on the survivability of the projectile.

REFERENCES

1. Backman, M.E. & Goldsmith, W. The mechanics of penetration of projectiles into targets. *J. Eng. Sci*., 1978, **16**, 1–99. doi: 10.1016/0020-7225(78)90002-2
2. Woodward, R.L.; Donnell, R.G. & Flockhart, C.J. Failure mechanisms in impacting penetrators. *J. Mater. Sci*., 1992, **27**, 6411–6416. doi: 10.1007/bf00576292
3. Rakvåg, K.G.; Børvik, T.; Westermann, I. & Hopperstad, O.S. An experimental study on the deformation and fracture modes of steel projectiles during impact. *Mater. Des*., 2013, **51**, 242-256. doi: 10.1016/j.matdes.2013.04.036
4. Chen, X.W.; Chen, G. & Zhang, F.J. Deformation and failure modes of soft steel projectiles impacting harder steel targets at increasing velocity. *Exp. Mech*., 2008, **48**, 335–354. doi: 10.1007/s11340-007-9110-4
5. Ren, Y.; Tan, C.; Zhang, J. & Wang, F. Dynamic fracture of Ti–6Al–4V alloy in Taylor impact test. *Trans. Nonferr. Metal. Soc*., 2011, **21**, 223–235. doi: 10.1016/s1003-6326(11)60703-6
6. Xiao, X.; Zhang, W.; Wei, G. & Mu, Z. Effect of projectile hardness on deformation and fracture behavior in the Taylor impact test. *Mater. Des*., 2010, **31**, 4913–4920. doi: 10.1016/j.matdes.2010.05.027
7. Domenico, V. & Francesco, G. Innovative technologies for controlled fragmentation warheads. *J. Appl. Mech*., 2013, **80**, 031704 1-5. doi: 10.1115/1.4023341
8. Shen, Z.X.; Yuan, H. & Li, Y.Z. Influence of localized melting on dynamic fracture behaviours of metallic shell. *Propell. Explos. Pyro*., 2017, **42**, 906-911. doi: 10.11776/cjam.33.05.D110
9. Børvik, T.; Hopperstad, O.S.; Berstad, T. & Langseth, M. A computational model of viscoplasticity and ductile damage for impact and penetration. *Eur. J. Mech. A/Solid*, 2001, **20**, 685–712. doi: 10.1016/s0997-7538(01)01157-3
10. Pradipta, K.J.; Bidyapati, M.; Kumar, K.S. & Balakrishna, B.T. An experimental study on the ballistic impact behavior of some metallic armour materials against 7.62 mm deformable projectile. *Mater. Des*., 2010, **31**, 3308-3316. doi:10.1016/j.matdes.2010.02.005
11. Zukas, J. A. & Schffler, D. R. Impact effects in multilayered plates. *Int. J. Solids. Struct*., 2001, **38**, 3321–3328. doi:10.1016/S0020-7683(00)00260-2
12. Chen, X.W.; Li, Q.M.; Zhang, F.J. & He, L.L. Investigation of the structural failure of penetration projectiles. *Int. J. Protective Structures*, 2010, **1**, 41-65. doi:10.1260/2041-4196.1.1.41
13. Mu, Z.C. & Zhang, W. An investigation on mass loss of ogival projectiles penetrating concrete targets. *Int. J. Impact Eng.* 2011, **38**, 770-778. doi:10.1016/j.ijimpeng.2011.04.002

ACKNOWLEDGMENT

The authors would like to thank the Impact Environmental Material Laboratory and the Subject of Zhejiang Provincial National Quality Infrastructure (NO. 20180119) for their financial supporting this present work.

CONTRIBUTORS

Dr Zhengxiang Shen, currently working in Ningbo Special Equipment Inspection & Research Institute, his research areas are failure prevention & analysis and engineering mechanics.
His contribution to the current study includes experiments implementation and paper writing.

Dr Hu Chen, currently working in Ningbo Special Equipment Inspection & Research Institute, his research area is mechanical engineering.
His contribution to the current study is experiments design.

Mr Du Wang, currently working in Ningbo Special Equipment Inspection & Research Institute, his research area is nondestructive testing.
His contribution to the current study is magnetic particle testing.

Mr Shuqiang Yuan, senior research fellow of China North Material Science and Engineering Technology Group, His research area is material processing engineering.
His contribution to the current study is re-melting of material by high energy beam.

Mr Dingyue Chen, senior engineer with the rank of a professor, currently working in Ningbo Special Equipment Inspection & Research Institute, his research area is mechanical engineering.
His contribution to the current study is establishing mathematical model.

Mr Guorong Zhu, senior engineer with the rank of a professor, currently working in Ningbo Special Equipment Inspection &Research Institute, his research area is failure analysis of structure.
His contribution to the current study is general technical guidance of this work.